



Design of Ag_3PO_4 for highly enhanced photocatalyst using hydroxyapatite as a source of phosphate ion

Uyi Sulaeman^{a,*}, Suhendar Suhendar^a, Hartiwi Diastuti^a, Anung Riapanitra^a, Shu Yin^b

^a Department of Chemistry, Jenderal Soedirman University, Purwokerto, 53123, Indonesia

^b Institute of Multidisciplinary Research for Advanced Materials, Tohoku University, Sendai, 980-8577, Japan

ARTICLE INFO

Keywords:

Defect sites
Hydroxyapatite
Phosphate ion
Photocatalyst
Silver orthophosphate

ABSTRACT

The effect of hydroxyapatite on structure, particle size, and band gap energy of silver orthophosphate (Ag_3PO_4) have been investigated. The hydroxyapatite as a source of phosphate ion was prepared using the coprecipitation of CaCl_2 and KH_2PO_4 . To produce the product of Ag_3PO_4 , the as-synthesized hydroxyapatite was suspended in water and quickly added to a silver nitrate solution. The obtained photocatalysts were characterized using XRD, SEM, DRS, and XPS. The high crystallinity of single phase Ag_3PO_4 was easily produced using the hydroxyapatite. Photocatalytic activities of the product were evaluated using RhB decomposition under blue light irradiation. The hydroxyapatite as a source of phosphate ion dramatically decreases the particle size and increases the absorption in the visible region. This obtained photocatalyst significantly improves the photocatalytic activity. The mechanism of reaction works in the following order: holes > superoxide radical > hydroxyl radical.

1. Introduction

Recently, the Ag_3PO_4 -based photocatalysts have attracted attention, because they have a low band gap and possessing high activities under visible light irradiation. The modification of these catalysts into the homojunction construction [1], Z-Scheme composite design [2], and defect generation [3] has enhanced their catalytic activity. Many researchers have mainly focused on Ag-based heterojunction in Ag_3PO_4 photocatalyst improvement. For example, the incorporation of reduced graphene oxide (RGO) into the $\text{BiPO}_4/\text{Ag}/\text{Ag}_3\text{PO}_4$ heterojunction improved the charge transfer and suppressed the recombination of electron/hole pairs [4]. The Z-scheme heterojunction and surface plasmon resonance effect could also be generated by the design of $\text{Ag}_3\text{PO}_4/\text{Ag}/\text{Ag}_2\text{MoO}_4$ [5]. This impressive design enhanced the photocatalytic activity and stability. Another photocatalyst, TiO_2 , could also be improved by forming the Ag quantum dots on TiO_2 . This modification could generate the surface plasmon resonance effect that improves the visible light photocatalytic activity [6]. However, the formation of metallic Ag could decrease the stability, for instance, the addition of Ti (IV) co-catalyst on AgBr decreases the stability because the accumulated electron in CB promotes the reduction of Ag^+ ions into metallic Ag [7]. This problem could be improved by surface modification using Fe(III) as an electron co-catalyst. The photocatalytic activity was not only affected by the Ag nanoparticle but also affected by phosphate ion.

The grafting of phosphate on the surface-phase junction structure of twinned BiPO_4 affected the position of energy band and improve the redox ability [8].

The outstanding properties of Ag_3PO_4 could be generated by modification of the starting material. The high activity of {111} facet could be created using the starting material of AgNO_3 and H_3PO_4 in ethanol [9,10]. The cauliflower-like spheres Ag_3PO_4 prepared by starting material of $(\text{NH}_4)_3\text{PO}_4$ showed high photocatalytic activity under visible light irradiation [11]. This preparation method decreases the particle size and suppresses the OH-related defects. Ag_3PO_4 nanoparticles, tetrahedrons, trisoctahedrons, and tetrapods could be designed by the synergetic reaction of Ag nanocrystals, phosphate anions and hydrogen peroxide (H_2O_2) [12]. The oxidizing ability of H_2O_2 affected the morphology and could be adjusted by the acidity and alkalinity of the reaction solution. The addition of tartaric acid to starting material could also shape the hollow microspheres that possess high surface area [13] and improve the catalytic activity. The approach of starting material modification is very challenging to obtain the properties of high catalytic activity. Therefore, it is possible that the new starting material of hydroxyapatite (HAP) is used as starting material for Ag_3PO_4 preparation.

In the photocatalysts, the HAP compound has been used as a composite material that enhanced catalytic activity. For instance, the HAP in TiO_2/HAP composites inhibit the phase transformation from anatase

* Corresponding author.

E-mail address: uyi_sulaeman@yahoo.com (U. Sulaeman).

<https://doi.org/10.1016/j.solidstatedciences.2018.09.015>

Received 6 July 2018; Received in revised form 17 September 2018; Accepted 30 September 2018

Available online 04 October 2018

1293-2558/ © 2018 Elsevier Masson SAS. All rights reserved.

to rutile of TiO₂ and prevented the formation of large TiO₂ agglomerates, leading to the higher dispersion of TiO₂ nanoparticles [14], consequently, the photocatalytic activity could be enhanced. The TiO₂/HAP composite could also enhance the capacity and weaken the intensity of HCHO adsorption [15]. The HAP/TiO₂ composite thin films prepared by sol-gel processes lead to the particle size of 10–25 nm [16]. Photocatalytic degradation of adsorbed aureomycin hydrochloride was also effective using the modified graphene oxide/nano-hydroxyapatite (CMGO/nHA) composite [17]. This band gap of graphene oxide increased from 1.7 to 2.8 eV by surface modification and composite formulation. The ZnO/HAP nanocomposites improved the rates of sorption of ciprofloxacin and ofloxacin [18]. The use of HAP in these photocatalyst designs reflected that HAP has a significant role.

The HAP could also be utilized to improve the catalytic activity of Ag₃PO₄ through the composite design. The Ag₃PO₄/HAP composite prepared by a facile in-situ ion exchange method significantly improved the separation of the photogenerated electron-hole pairs [19]. This excellent catalytic performance may be related to the vacancy of HAP and Z-scheme mechanism that generated in the composite. A new HAP/N-doped carbon dots/Ag₃PO₄ composite prepared by a hydrothermal method could improve the photocatalytic performance [20]. This high activity originated from the synergetic effects of HAP, carbon dots and the Ag₃PO₄.

The new approach of HAP application in the Ag₃PO₄ synthesis has been proposed in this work. HAP is not only used in the composite design but also as an agent for particle size control. Here, HAP was used as a source of phosphate ion in Ag₃PO₄ synthesis. The HAP synthesized by CaCl₂ and KH₂PO₄ was suspended in water and added to a silver nitrate solution to form the yellow crystalline of Ag₃PO₄. This new method successfully decreases the particle size and generates the defect sites on the surface that improve the photocatalytic activity. The main species of mechanism was changed from the superoxide ion radical to the holes mechanism.

2. Experimental

2.1. Synthesis of HAP

The hydroxyapatite (Ca₁₀(PO₄)₆(OH)₂/HAP) was synthesized using the co-precipitation method of CaCl₂ and KH₂PO₄ [21]. The pH of the CaCl₂ solution (1 M) and KH₂PO₄ solution (0.6 M) were maintained at 8 using the ethylenediamine. An amount of 100 mL of KH₂PO₄ solution, was stirred at room temperature, then added with 100 mL of CaCl₂ solution dropwise for 60 min to obtain the white solid of HAP. This suspension was aging for 12 h, and the precipitate was filtered and washed with water three times and dried in the oven at 60 °C for 12 h.

2.2. Synthesis and characterization of Ag₃PO₄

The Ag₃PO₄ was prepared with two different phosphate ion sources of HAP and KH₂PO₄. The Ag₃PO₄ synthesized using HAP as a source of phosphate ion were namely Ag₃PO₄/HAP. Typically, in amounts of 0.3 g of HAP were added to the 20 mL of water (and stirred for 5 min to obtain HAP suspension). The AgNO₃ solution (1.0195 g) in 10 mL of water) was quickly added to the HAP suspension (and stirred 30 min to obtain the yellow precipitate of catalyst). The product was filtered, washed with water then dried in the oven at 60 °C for 2 h. The sample without HAP was also prepared. Typically, at the amount of 0.245 g of KH₂PO₄ was added to 20 mL of water. The AgNO₃ solution (1,0195 g) in 10 mL of water) was added quickly to the KH₂PO₄ solution. The product was filtered, washed with water then dried in the oven at 60° for 2 h. The sample of Ag₃PO₄ and Ag₃PO₄/HAP were characterized using the XRD (Shimadzu 7000), DRS (JASCO V-670), and SEM (JEOL JSM 6510LA). The core level of Ag₃PO₄/HAP was investigated using XPS (Perkin Elmer PHI 5600).

2.3. Photocatalytic evaluation

The photocatalytic activities were evaluated under blue light irradiation [3]. The amount of 0.1 g catalysts was added to 100 mL of RhB solution (10 mg/L) and equilibrated for 20 min. The photocatalytic reaction was done under the blue light irradiation (Duralux, 3 Watt). The 5 mL of sample was taken out and centrifuged to separate the solution from the catalyst and the concentration of RhB was determined by the spectrophotometer (Shimadzu 1800). The stability of the catalyst was also evaluated up to 4 cycles of photocatalytic reaction.

2.4. Mechanism of photocatalysis

The three solutions of 10 mg/L RhB with the volume of 100 mL were each added by isopropyl alcohol (IPA), ammonium oxalate (AO) and p-benzoquinone (BQ), respectively [3]. Their concentration was designed at 0.1 mmol/L. Under magnetic stirring, an amount of 0.1 g catalysts added to the solution. The photocatalytic reaction was carried out under blue light irradiation and the concentration of RhB was measured by the spectrophotometer.

3. Results and discussion

The Ag₃PO₄ photocatalyst was successfully synthesized using the HAP as a source of phosphate ion. The structure of the body-centered cubic structure (JCPDS No. 06–0505) was observed in both the Ag₃PO₄ and Ag₃PO₄/HAP (Fig. 1) [22]. The strongest three peaks of 33.307°, 36.591°, and 55.028° found in the sample of Ag₃PO₄ (without HAP) originated from the (2 1 0), (2 1 1), and (3 2 0) crystal planes, respectively. In the sample of Ag₃PO₄/HAP, the strongest three peaks were shifted to 33.326°, 36.609 and 55.040 for the crystal plane of (2 1 0), (2 1 1), and (3 2 0), respectively. At the peak of (2 1 1) crystal plane, the FWHM of 0.081° was observed in Ag₃PO₄ and 0.121° in Ag₃PO₄/HAP. The shift of 2theta and higher of FWHM in Ag₃PO₄/HAP sample might be the effect of calcium doping in the lattice. The crystallinity of Ag₃PO₄/HAP (97.7%) is higher than that of Ag₃PO₄ (95.3%). No others XRD peak was observed on the samples, indicating that the samples were single phase. From these results, it could be concluded that the HAP did not form a composite with the Ag₃PO₄. The HAP was only providing the phosphate ion in the synthesis of Ag₃PO₄.

Fig. 2 showed the absorption of Ag₃PO₄ and Ag₃PO₄/HAP. They absorb solar energy with a wavelength shorter than ~530 nm. The higher absorption above 500 nm was found on the Ag₃PO₄/HAP, indicating that the defect site might be formed on the surface. The band

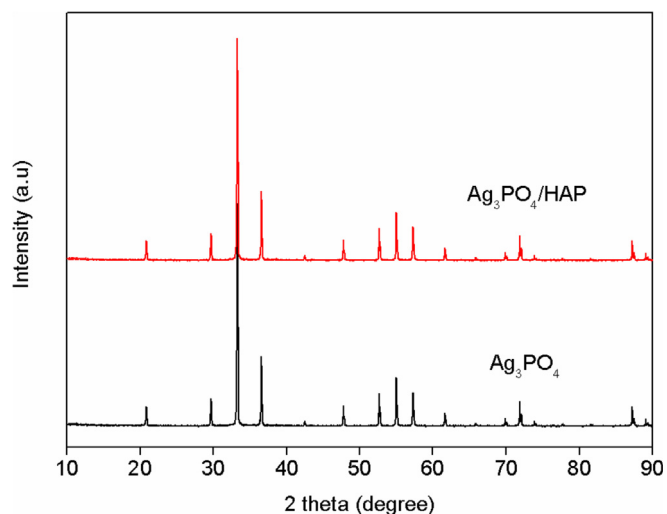


Fig. 1. XRD profile of Ag₃PO₄ (synthesized using KH₂PO₄) and Ag₃PO₄/HAP (synthesized using hydroxyapatite).

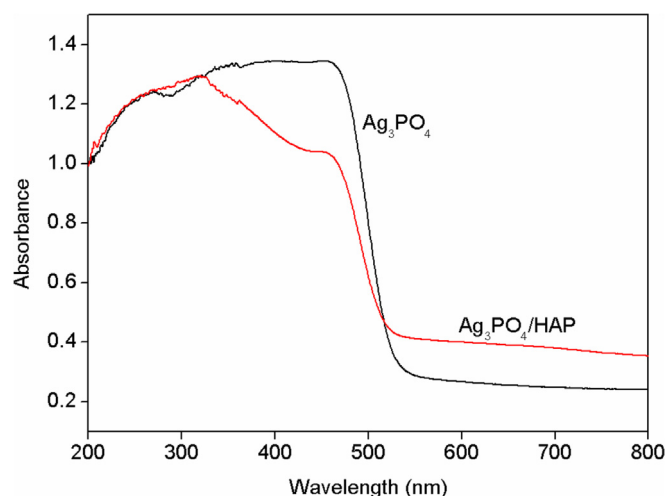


Fig. 2. DRS of Ag_3PO_4 (synthesized using KH_2PO_4) and $\text{Ag}_3\text{PO}_4/\text{HAP}$ (synthesized using hydroxyapatite).

gap of 2.43 eV and 2.40 eV was obtained in the sample of Ag_3PO_4 and $\text{Ag}_3\text{PO}_4/\text{HAP}$, respectively.

The morphology and particle size of Ag_3PO_4 and $\text{Ag}_3\text{PO}_4/\text{HAP}$ were investigated using SEM (Fig. 3). The large particle of 3–5 μm was obtained when Ag_3PO_4 synthesized using KH_2PO_4 as a source of phosphate ion. When the HAP was used as a source of phosphate ion, the small particle of 0.4–1.2 μm was obtained, indicating that the use of HAP as the precursor is a crucial factor to form a smaller particle size. After adding with AgNO_3 , the suspension of HAP changed into the yellow crystalline. It indicates that the phosphate in HAP reacted with Ag^+ ion resulting in Ag_3PO_4 . The Ca^{2+} of HAP dissolved to the solution and can be cleaned by washing treatment.

The core level of $\text{Ag}_3\text{PO}_4/\text{HAP}$ was investigated using the XPS and the results were shown in Fig. 4. The element of Ag, P, O was clearly detected and shown in the survey of XPS (Fig. 4(a)). The binding energy (BE) of 373.8 eV and 367.8 eV were assigned to the $\text{Ag}3d_{3/2}$ and $\text{Ag}3d_{5/2}$, respectively (Fig. 4(b)). The BE of 132.9 eV was assigned to P2p (Fig. 4(c)). There are two types of oxygen on $\text{Ag}_3\text{PO}_4/\text{HAP}$ (O-1 and O-2) (Fig. 4(d)). The BE of 530.5 eV (O-1) suggested that the oxygen originated from the non-bridging (P=O) oxygen atoms of Ag_3PO_4 , whereas at the BE of 532.4 eV, the oxygen originated from the bridging oxygen atoms (P–O–Ag) [23]. The carbon impurities were observed in $\text{Ag}_3\text{PO}_4/\text{HAP}$ (Fig. 4(e)). The BEs of 284.4 eV (C1) and 285.1 eV (C2) assigned to sp^2 and sp^3 hybridized C atom, respectively, whereas the small peak energy of 286.6 eV (C3) and 288.5 eV (C4) might be originated from C–O and COOH, respectively [24]. These types of carbons appeared due to a synthesis of samples under air condition. The as-synthesized HAP might have an impurity of ethylenediamine that generates the sp^2 and sp^3 hybridized C atom on the surface of Ag_3PO_4 . These phenomena occur during the coprecipitation reaction of phosphate ion and silver ion. A small concentration of Ca2p (4.2%) was detected in the XPS measurement (Fig. 4(f)), indicating that the calcium

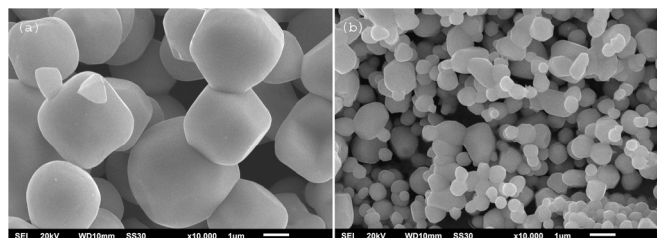


Fig. 3. SEM images of Ag_3PO_4 (a) prepared by KH_2PO_4 and $\text{Ag}_3\text{PO}_4/\text{HAP}$ (b) prepared by hydroxyapatite as a source of phosphate ion.

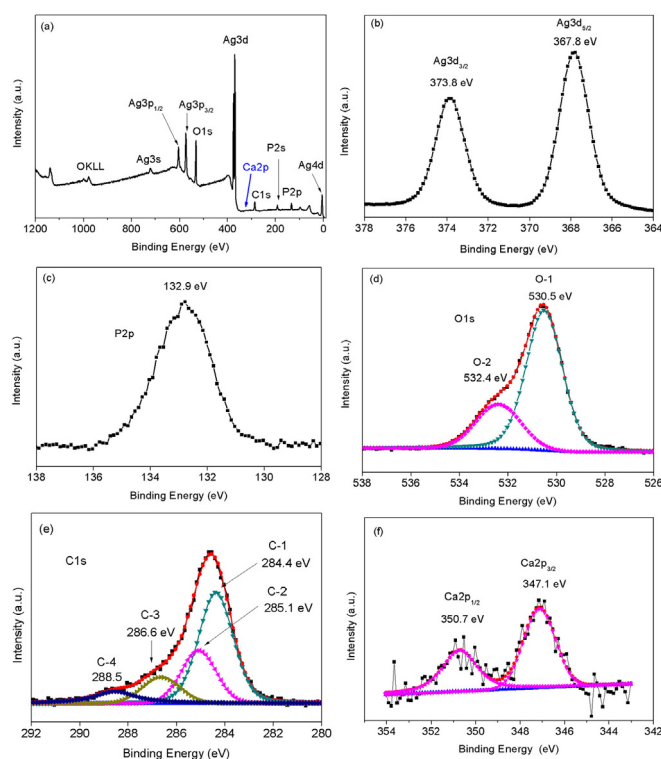


Fig. 4. XPS survey (a), Ag3d (b), P2p(c), O1s (d), C1s (e), and Ca2p (f) of $\text{Ag}_3\text{PO}_4/\text{HAP}$ sample prepared by hydroxyapatite before photocatalytic reaction.

doped on the surface of Ag_3PO_4 . It indicates that the composite of $\text{Ag}_3\text{PO}_4/\text{HAP}$ was not created, only Ca doping might occur on the sample. It is consistent with the XRD results. The HAP acted as a source of phosphate ion in the Ag_3PO_4 formation and has a significant role in controlling the growth particle.

Fig. 5 showed the photocatalytic activity of Ag_3PO_4 and $\text{Ag}_3\text{PO}_4/\text{HAP}$. The photocatalytic activity has followed the pseudo-first-order kinetics with the rate constant of 0.109 min^{-1} and 0.384 min^{-1} found in the Ag_3PO_4 and $\text{Ag}_3\text{PO}_4/\text{HAP}$, respectively [3]. The Ag_3PO_4 synthesized using HAP showed high photocatalytic activity, around 3.5 times higher compared to the Ag_3PO_4 synthesized using the KH_2PO_4 . The high photocatalytic activity might be caused by smaller particle size that has a relatively higher specific surface area [25]. The higher

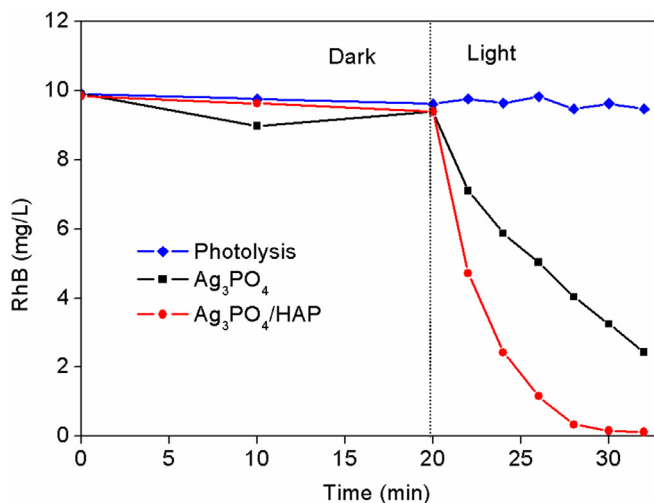


Fig. 5. Photocatalytic activity of Ag_3PO_4 (synthesized using KH_2PO_4) and $\text{Ag}_3\text{PO}_4/\text{HAP}$ (synthesized using hydroxyapatite).

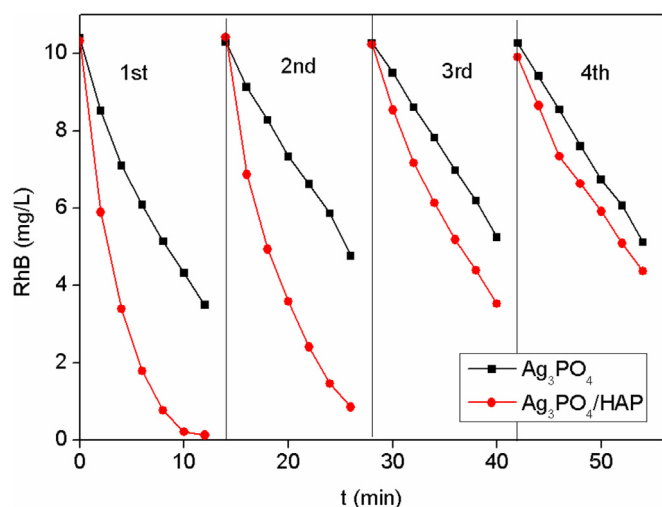


Fig. 6. Recycle experiments of RhB degradation by the Ag_3PO_4 synthesized using KH_2PO_4 and $\text{Ag}_3\text{PO}_4/\text{HAP}$ (synthesized using hydroxyapatite).

the photocatalyst surface area, the higher the absorption that contributes to the photocatalytic reaction [26]. It is also possible that the $\text{Ag}_3\text{PO}_4/\text{HAP}$ has a defect site due to having a high absorption above 500 nm as shown in Fig. 2. The previous results showed that the native defect of silver vacancy was observed in the sample that has high absorption in the visible region [3]. The defect sites might act as capture centers for the photoexcited electron that effectively suppress the recombination of electron and holes.

To evaluate the stability, the recycle experiments of RhB degradation up to 4 times were done (Fig. 6). The photocatalytic stability of $\text{Ag}_3\text{PO}_4/\text{HAP}$ was decreased significantly. However, the ability of photocatalysis at $\text{Ag}_3\text{PO}_4/\text{HAP}$ is higher than that of Ag_3PO_4 for all cycle catalytic reaction. To investigate the effect of photocatalytic reaction, the photocatalyst of $\text{Ag}_3\text{PO}_4/\text{HAP}$ after 4 cycles test was analyzed using the XPS. The results were shown in Fig. 7. The deconvolution of Ag3d showed that the BE of 374.2 eV and 368.5 eV were observed (Fig. 7(a)), indicating that the Ag^0 was formed on the surface [27]. This formation was generated by the photoreduction of Ag^+ to Ag^0 during the photocatalytic reaction. The decreased BE of P2p (132.1 eV) was also observed after photocatalytic reaction suggesting that the chemical environment of P2p has changed (Fig. 7(b)). The peak of O1s was deconvoluted into three peaks of 529.5 eV, 531.2 eV, and 533.1 eV (Fig. 7(c)). The BE of 529.5 eV was assigned to the lattice oxygen atom of Ag_3PO_4 [28], whereas the BE of 531.2 eV and 533.1 eV were assigned to the $\text{O}=\text{C}-\text{OH}$ and $\text{C}-\text{O}$, respectively [29]. The high intensity of 531.2 eV might also be coincident with the chemisorbed water or surface hydroxyl group [30,31]. These suggested that the catalyst after cyclic test might adsorb the product of RhB degradation. The BE of 284.4 eV, 285.6 eV, 286.9 eV, and 288.2 eV at C1s assigned to sp^2 , sp^3 hybridized C atom, $\text{C}-\text{O}$, and COOH respectively (Fig. 7(d)) [19]. The concentration of C1s after the cyclic test was higher compared to before cyclic test, suggesting that the carbon compounds from the RhB degradation highly adsorbed on the surface of $\text{Ag}_3\text{PO}_4/\text{HAP}$ (Table 1). The N1s and Cl2p were also identified in the sample (Fig. 7(e,f)), indicating that the products of RhB degradation contain nitrogen and chlorine adsorbed on to the surface of Ag_3PO_4 . The peak with the BE of 399.7 eV at N1s was assigned to C-N configuration [32,33]. The BE of 197.5 eV and 199.5 eV were assigned to $\text{Cl } 2p_{3/2}$ and $2p_{1/2}$ spin-orbit doublet [34], respectively.

The mechanisms of photocatalytic were evaluated using the scavengers of IPA, BQ, and AO to trap the species of $\cdot\text{OH}$, $\cdot\text{O}_2^-$, and h^+ , respectively. The results were shown in the Fig. 8. The different mechanism of the two samples was observed. In the Ag_3PO_4 system, the BQ scavenger strongly suppresses the photocatalytic reaction,

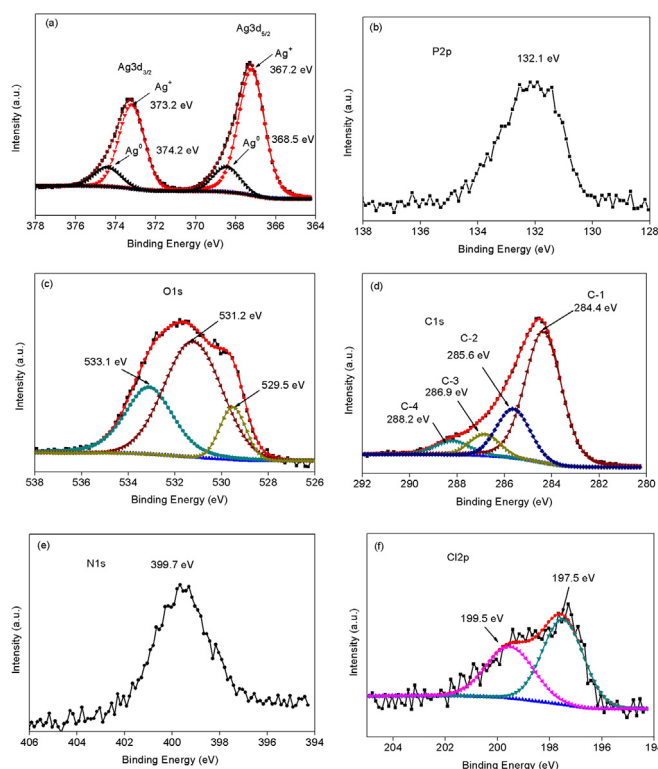


Fig. 7. The XPS analysis of Ag3d (a), P2p(b), O1s (c), C1s (d), N1s (e) and Cl2p (f) of $\text{Ag}_3\text{PO}_4/\text{HAP}$ sample prepared by hydroxyapatite after the photocatalytic reaction.

Table 1
Atomic concentration of $\text{Ag}_3\text{PO}_4/\text{PAH}$ before and after the cyclic test.

Treatment	Atomic concentration (%)						
	Ag 3d	P 2p	O 1s	C 1s	N 1s	Cl 2p	Ca 2p
Before cyclic test	25.89	11.05	42.68	19.97	0.00	0.00	0.41
After cyclic test	10.20	2.30	22.23	60.44	4.33	0.50	0.00

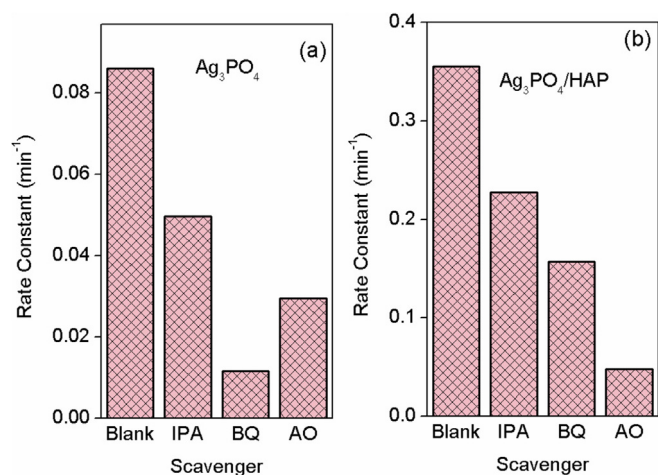


Fig. 8. Mechanism of photocatalytic activity in the system of Ag_3PO_4 (a) prepared by KH_2PO_4 and $\text{Ag}_3\text{PO}_4/\text{HAP}$ (b) prepared by hydroxyapatite as a source of phosphate ion.

indicating that the reaction mostly works via $\cdot\text{O}_2^-$, whereas in the $\text{Ag}_3\text{PO}_4/\text{HAP}$ system, the AO scavenger strongly suppresses the photocatalytic reaction, indicating that the h^+ is the main role of its

mechanism. The mechanism of active species in the Ag_3PO_4 works in the following order: $\cdot\text{O}_2^- > \text{h}^+ > \cdot\text{OH}$ and it was changed into the following order: $\text{h}^+ > \cdot\text{O}_2^- > \cdot\text{OH}$ in the $\text{Ag}_3\text{PO}_4/\text{HAP}$. The different mechanism might be caused by the different properties of the Ag_3PO_4 surface. Due to the higher carbon on the surface of the sample after the photocatalytic reaction (Table 1), the interaction of RhB–holes might be dominant in the reaction. It was consistent with the mechanism study that was dominated by holes. This interaction subsequently enhances the photocatalytic activity.

4. Conclusions

The single phase of Ag_3PO_4 was successfully synthesized using the hydroxyapatite (HAP) as a source of phosphate ion. The preparation of Ag_3PO_4 using the HAP ($\text{Ag}_3\text{PO}_4/\text{HAP}$) decreases the particle size and generates the high absorption in the visible region. The photocatalytic activity of $\text{Ag}_3\text{PO}_4/\text{HAP}$ increases up to 3.5 times higher compared to the Ag_3PO_4 . The mechanism of primary active species in the Ag_3PO_4 system works in the following order: $\cdot\text{O}_2^- > \text{h}^+ > \cdot\text{OH}$ and it was changed into the following order: $\text{h}^+ > \cdot\text{O}_2^- > \cdot\text{OH}$ in the $\text{Ag}_3\text{PO}_4/\text{HAP}$.

Acknowledgment

This research was supported by the Ministry of Research, Technology and Higher Education of the Republic of Indonesia in the Scheme of International Research Collaboration, Contract Number: 059/SP2H/LT/DRPM/2018. It was also partly supported by the JSPS KAKENHI Grant Number JP16H06439 (Grant-in-Aid for Scientific Research on Innovative Areas), the Dynamic Alliance for Open Innovation Bridging Human, Environment and Materials, the Cooperative Research Program of “Network Joint Research Center for Materials and Devices”.

References

- [1] Y. Xie, S. Luo, H. Huang, Z. Huang, Y. Liu, M. Fang, X. Wu, X. Min, *Colloids Surf. A Physicochem. Eng. Asp.* 546 (2018) 99–106.
- [2] M. You, J. Pan, C. Chi, B. Wang, W. Zhao, C. Song, Y. Zheng, C. Li, *J. Mater. Sci.* 53 (2018) 1978–1986.
- [3] U. Sulaeman, D. Hermawan, R. Andreas, A.Z. Abdullah, S. Yin, *Appl. Surf. Sci.* 428 (2018) 1029–1035.
- [4] N. Mohaghegh, E. Rahimi, *Solid State Sci.* 56 (2016) 10–15.
- [5] H. Tang, Y. Fu, S. Chang, S. Xie, G. Tang, *Chin. J. Catal.* 38 (2017) 337–347.
- [6] X. Yu, L. Shang, D. Wang, L. An, Z. Li, J. Liu, J. Shen, *Solid State Sci.* 80 (2018) 1–5.
- [7] H. Yu, W. Chen, X. Wang, Y. Xu, J. Yu, *Appl. Catal., B* 187 (2016) 163–170.
- [8] Y. Guo, P. Wang, J. Qian, Y. Ao, C. Wang, J. Hou, *Appl. Catal., B* 234 (2018) 90–99.
- [9] B. Zheng, X. Wang, C. Liu, K. Tan, Z. Xie, L. Zheng, *J. Mater. Chem. A* 1 (2013) 12635–12640.
- [10] U. Sulaeman, F. Febiyanto, S. Yin, T. Sato, *Catal. Commun.* 85 (2016) 22–25.
- [11] X. Song, R. Li, M. Xiang, S. Hong, K. Yao, Y. Huang, *Ceram. Int.* 43 (2017) 4692–4701.
- [12] F. Pang, X. Liu, M. He, J. Ge, *Nano Res* 8 (2015) 106–116.
- [13] L. Wang, L. Wang, D. Chu, Z. Wang, Y. Zhang, J. Su, *Catal. Commun.* 88 (2017) 53–55.
- [14] J. Guo, F. Dong, S. Zhong, B. Zhu, W. Huang, S. Zhang, *Catal. Lett.* 148 (2018) 359–373.
- [15] M. Hu, Z. Yao, X. Liu, L. Ma, Z. He, X. Wang, *J. Taiwan Inst. Chem. Eng.* 85 (2018) 91–97.
- [16] K. Kaviyarasu, A. Mariappan, K. Neyvasagamd, A. Ayeshamariame, P. Pandi, R.R. Palanichamy, C. Gopinathan, G.T. Mola, M. Maaza, *Surf. Interface* 6 (2017) 247–255.
- [17] T.S. Anirudhan, J.R. Deepa, A.S. Nair, *J. Ind. Eng. Chem.* 47 (2017) 415–430.
- [18] C. El Bekkali, H. Bouyarmene, M. El Karbane, S. Masse, A. Saoiabi, T. Coradin, A. Laghzizil, *Colloids Surf. A Physicochem. Eng. Asp.* 539 (2018) 364–370.
- [19] Y. Chai, J. Ding, L. Wang, Q. Liu, J. Ren, W. Dai, *Appl. Catal., B* 179 (2015) 29–36.
- [20] Q. Chang, X. Meng, S.L. Hu, F. Zhang, J.L. Yang, *RSC Adv.* 7 (2017) 30191–33019.
- [21] J.D. Wang, J.K. Liu, Y. Lu, D.J. Hong, X.H. Yang, *Mater. Res. Bull.* 55 (2014) 190–195.
- [22] X. Cui, L. Tian, X. Xian, H. Tang, X. Yang, *Appl. Surf. Sci.* 430 (2018) 108–115.
- [23] P. Dong, G. Hou, C. Liu, X. Zhang, H. Tian, F. Xu, X. Xi, R. Shao, *Materials* 9 (2016) 968.
- [24] F. Zhao, A. Vrajitoarea, Q. Jiang, X. Han, A. Chaudhary, J.O. Welch, R.B. Jackman, *Sci. Rep.* 5 (2015) 13771.
- [25] A. Nakada, A. Saeki, M. Higashi, H. Kageyama, R. Abe, *J. Mater. Chem. A* 6 (2018) 10909–10917.
- [26] L. Jing, Z. Xu, X. Sun, J. Shang, W. Chai, *Appl. Surf. Sci.* 180 (2001) 308–314.
- [27] F. Chen, Q. Yang, X. Li, G. Zeng, D. Wang, C. Niu, J. Zhao, H. An, T. Xie, Y. Deng, *Appl. Catal., B* 200 (2017) 330–342.
- [28] Z. Zhang, J. Long, X. Xie, H. Zhuang, Y. Zhou, H. Lin, R. Yuan, W. Dai, Z. Ding, X. Wang, X. Fu, *Appl. Catal.* 425–426 (2012) 117–124.
- [29] Y.J. Oh, J.J. Yoo, Y.I. Kim, J.K. Yoon, H.N. Yoon, J.H. Kim, S.B. Park, *Electrochim. Acta* 116 (2014) 118–128.
- [30] L. Ge, *Mater. Chem. Phys.* 107 (2008) 465–470.
- [31] S. Halevy, Y. Boichlin, Y. Kadosh, A. Kaplan, H. Avraham, A. Nissim, R. Ben Hamo, T. Ohaion-Raz, E. Korin, A. Bettelheim, *Sci. Rep.* 7 (2017) 4987.
- [32] Q. Cao, L. Xiao, J. Li, C. Cao, S. Li, J. Wang, *Powder Technol.* 292 (2016) 186–194.
- [33] H. Hunke, N. Soin, T.H. Shah, E. Kramer, A. Pascual, M.S.L. Karuna, E. Siores, *Materials* 8 (2015) 2258–2275.
- [34] B.L. Oliva-Chatelain, A.R. Barron, *AIMS Mater. Sci.* 3 (2016) 1–21.



ScienceDirect

Journals & Books



Register

Sign in



Solid State Sciences

Supports *open access*

3.059

Impact Factor

Articles & Issues ▾

About ▾

Publish ▾

Order journal ↗

🔍 Search in this journal

Submit your article ↗

Guide for authors ↗

Volume 86

Pages 1-110 (December 2018)

← Previous vol/issue

Next vol/issue >

Solid State Sciences
incorporating
International Journal of Inorganic Materials
www.elsevier.com/locate/ssscie

Editor-in-chief

M. Drillon

Institut de Physique et Chimie des Matériaux de Strasbourg
23 rue du Loess, 67034 Strasbourg, France
drillon@ipcms.u-strasbg.fr

European Editor

B. Albert

Eduard-Zintl-Institute of Inorganic and
Physical Chemistry
Technical University of Darmstadt
Alarich-Weiss-Str. 12, 64287
Darmstadt, Germany
albert@ac.chemie.tu-darmstadt.de

North American Editor

M. Subramanian

Department of Chemistry,
Oregon State University
Corvallis, OR 97331-4003, USA
Mas.subramanian@oregonstate.edu

Asian Editor

Sang Woo Han

Department of Chemistry,
KAIST Daejeon, 305-701, Korea
sangwoohan@kaist.ac.kr

Advisory Editorial Board

G. Ferey (Founding Editor) *France*

M. Jansen (Founding Editor)
Germany

M. Takano (Founding Editor)
Japan

M. Alario-Franco *Spain*

E. Antipov *Russia*

J.P. Attfield *UK*

S. Bals *Belgium*

J. Chen *China*

J. Yu *China*

J.H. Choy *Korea*

E. Coronado *Spain*

J. Etourneau *France*

C. Grey *USA*

A.J. Jacobson *USA*

M. Karppinen *Finland*

S. Lidin *Sweden*

J. Livage *France*

J. Lucas *France*

A. Maignan *France*

G. Meyer *USA*

A. Müller *Germany*

L. Nazar *Canada*

D. O'Hare *UK*

M. Pouchard *France*

C.N.R. Rao *India*

B. Raveau *France*

M. Ribes *France*

J. Rocha *Portugal*

H.W. Roesky *Germany*

R. Seshadri *USA*

A. Simon *Germany*

A. Sleight *USA*

J.M. Tarascon *France*

R. Tenne *Israel*

J. Thackeray *Canada*

J.M. Thomas *UK*

M. Tournoux *France*

A. Weidenkaff *Germany*

A.K. West *UK*

Y. Xi *China*

R. Xu *China*

O. Yaghi *USA*

M. Yoshimura *Japan*

H. zur Loye *Columbia*

Submit your article

Menu



Search in this journal

Volume 86

Pages 1-110 (December 2018)

[Download full issue](#)

[< Previous vol/issue](#)

[Next vol/issue >](#)

Receive an update when the latest issues in this journal are published

[Sign in to set up alerts](#)

Full text access

Editorial Board

Page ii

[Download PDF](#)

Research article Abstract only

Design of Ag_3PO_4 for highly enhanced photocatalyst using hydroxyapatite as a source of phosphate ion

Uyi Sulaeman, Suhendar Suhendar, Hartiwi Diastuti, Anung Riapanitra, Shu Yin

Pages 1-5

[Purchase PDF](#)

Article preview

FEEDBACK

Submit your article

Menu



Search in this journal

Research article Abstract only

Influence of carbon source on the anatase and brookite mixed phase of the C-doped TiO₂ nanoparticles and their photocatalytic activity

Yingwen Duan, Xinwei Chen, Xiangxiang Zhang, Wan Xiang, Chunfang Wu

Pages 12-18

[Purchase PDF](#) [Article preview](#)

Research article Abstract only

Formation mechanism of Sialon in alumina-ferro-silicon-nitride composite under nitrogen atmosphere at high temperatures

Xi Nie, Yong Li, Peng Jiang, Haixia Qin

Pages 19-23

[Purchase PDF](#) [Article preview](#)

Research article Abstract only

Synthesis, characterization and CO₂ adsorption of NaA, NaX and NaZSM-5 from rice husk ash

Yisong Wang, Tao Du, He Jia, Ziyang Qiu, Yanli Song

Pages 24-33

[Purchase PDF](#) [Article preview](#)

Research article Abstract only

Electronic structure of $Ce_{1-x}M_xO_2$, where $M = Rh, Pd$, by MBJLDA calculations

Maciej J. Winiarski, Michalina Kurnatowska

Pages 34-37

[Purchase PDF](#) [Article preview](#)

Research article Abstract only

Assignment of the electronic transitions in B_{4,3}C boron carbide implies a specifically distorted crystal structure

Helmut Werheit

Pages 38-44

[Purchase PDF](#) [Article preview](#)

Submit your article

Menu



Search in this journal

Research article Abstract only

Synthesis of $\text{Co}_3\text{O}_4/\text{CoOOH}$ via electrochemical dispersion using a pulse alternating current method for lithium-ion batteries and supercapacitors

Daria Chernysheva, Codruta Vlaic, Igor Leontyev, Lyudmila Pudova, ... Nina Smirnova

Pages 53-59

[Purchase PDF](#) Article preview

Research article Abstract only

Theoretical insight into structural and electronic properties of cationic Sc_n^+ ($n=2-13$): A benchmark study

Saira Sajjad, Tariq Mahmood, Ralf Ludwig, Khurshid Ayub

Pages 60-68

[Purchase PDF](#) Article preview

Research article Abstract only

An insight into the structure, conductivity and ion dynamics of Sr-Sm co-doped ceria oxygen ion conductors: Effect of defect interaction

Sk. Anirban, Abhigyan Dutta

Pages 69-76

[Purchase PDF](#) Article preview

Research article Abstract only

Synthesis, crystal structure, vibrational, optical properties, thermal analysis and theoretical study of a new Sn(IV) complex $(\text{C}_5\text{H}_{14}\text{N}_2)_2[\text{SnCl}_6]_2 \cdot 5\text{H}_2\text{O}$

S. BelhajSalah, M.S.M. Abdelbaky, S. García-Granda, K. Essalah, ... M.L. Mrad

Pages 77-85

[Purchase PDF](#) Article preview

Research article Abstract only

Structural and magnetic properties of nanocrystalline nickel ferrite (NiFe_2O_4) synthesized in sol-gel and combustion routes

B.B.V.S. Vara Prasad, K.V. Ramesh, Adiraj Srinivas

Submit your article

Menu

 Search in this journal

V. Ganesh, L. Haritha, Mohd Anis, Mohd Shkir, ... S. AlFaify

Pages 98-106


 [Purchase PDF](#) Article preview 

Research article Abstract only

Magnetic field induced anomalous Core-Shell magnetic behavior in short-rod Co_3O_4

Wenjian Fang, Zeyun Fan, Wei Lei, Xiaodong Si, ... Yongsheng Liu

Pages 107-110

 [Purchase PDF](#) Article preview 

Full text access

Graphical abstract TOC

Page IBC

 [Download PDF](#)

Full text access

Graphical abstract TOC

Page OBC

 [Download PDF](#)

 [Previous vol/issue](#)

[Next vol/issue](#) 

ISSN: 1293-2558

Copyright © 2022 Elsevier Masson SAS. All rights reserved

